Mon. Not. R. Astron. Soc. **000**, 000–000 (0000) Printed 27 February 2013 (MN LATEX style file v2.2)

Effects of rotation on the Lyman-α line morphology in distant galaxies

Nicolas Garavito-Camargo.[1] Jaime E. Forero-Romero[2]

[1] *Uni A* [2] *Uni B*

27 February 2013

ABSTRACT

Key words: galaxies: high-redshift - galaxies: star formation - line: formation

1 INTRODUCTION

Due to the resonant nature of the lyman alpha line, gas kinematics play an important role shaping its morphology. In the literature there has been extensive studies of outflow/inflow configurations.

In this paper we study for the first time the impact of rotation on the morphology of the Lyman α line. To isolate the effects of rotation we focus on a simple system: the gas distribution is spherical, with homogenous density and the gas rotates as a solid body.

This paper is paper is structured as follows.

2 IMPLEMENTATION OF BULK GAS ROTATION

We implement into CLARA the simplest model whereby a sphere rotates with homogeneous angular velocity. We define a cartesian coordinate system with its origin at the center of the sphere and the rotation axis to be the z-axis, the components in the bulk velocity field, $\vec{v} = v_x\hat{i} + v_y\hat{j} + v_z\hat{k}$. in the gas can be written as

$$v_x = -\frac{y}{R}V_{\max}, \tag{1a}$$

$$v_y = \frac{x}{R}V_{\max}, \tag{1b}$$

$$v_z = 0, \tag{1c}$$

where R is the radius of the sphere and $V_{\max}$ is the linear velocity at the sphere's surface. The minus sign in the x-component of the velocity indicates the direction of rotation, in this case we assume that the angular velocity vector goes in the $\hat{k}$ direction. The linear dependence of the velocity on the radial distance describes the case of constant angular velocity $\omega = V_{\max}/R$.

We take the polar angle θ that a unitary vector makes with the rotation axis as defined by the dot product $\cos\theta = \hat{u}\cdot\hat{k}$. In the Section 4 we will present in detail how the line differs at different observing angles θ.

Velocity (km s^{-1})	$V_{\max}$	0, 50, 100, 200, 300
Hydrogen Optical Depth	τ_H	10^5, 10^6, 10^7
Dust Optical Depth	τ_A	XXX
Photons Distributions		Central, Homogeneous

Table 1. Values for the varying input parameters in CLARA. Taking into account all the possible combinations for these models

3 GRID OF SIMULATED MODELS

We compute the emergent Lyman-α line for several models with differents values for the maximal rotational velocity, hydrogend optical depth, dust optical depth and initial distributions of the photons with respect to the gas. There are in total 60 models with the input parameters summarized in Table 1.

4 RESULTS

The central result of this paper is summarized in Figure 4 where we show that rotation as a considerable effect on the morphology of the emergent Lyman-alpha line both in the case where the photons are emitted at the sphere's center and when they are initialized with an homogeneous distribution all over the gas volume.

The results for this outgoing spectra are integrated over the whole sphere, meaning that all the escaping photons were taking into account regardless of the direction of the outgoing photons. Figure 2 shows how if one gives a weight to each outgoing photon according to its direction when escaping the gas distribution it is posible to detect notable differences in the spectrum for different viewing angles.

4.1 Maximums Position

Maximums position provides information about the wave length of the majority of the outgoing photons after they interact with the gas cloud, as a photon escapes with more

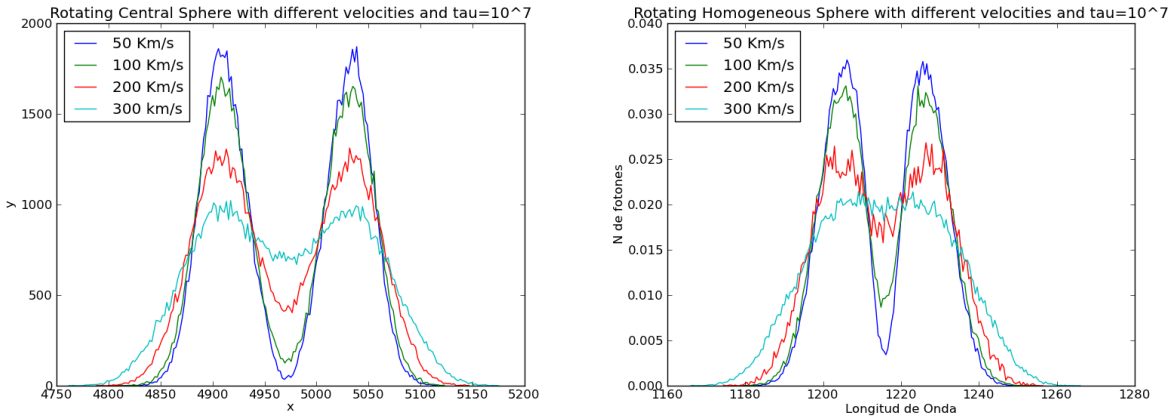

Figure 1. Shape of the lyman alpha line for differents velocities. The left (right) panel shows the central (homogeneous) photon distribution.

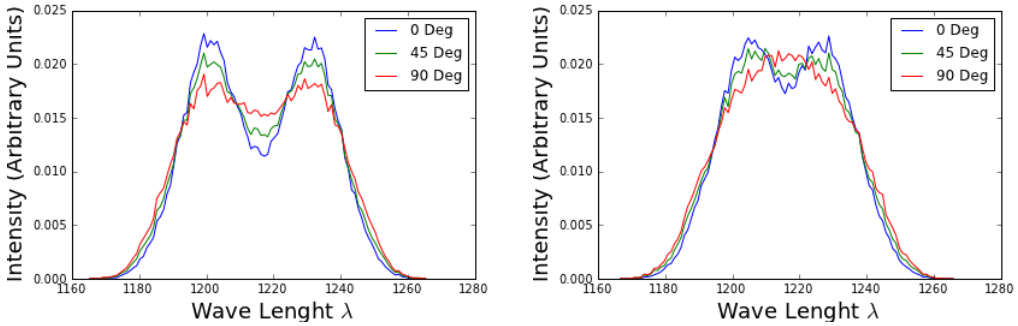

Figure 2. Spectra for different observers. Model:$V = 300\,\mathrm{km\ s^{-1}}$, Optical Depth $\tau = 10^7$ and Central Distribution without dust.

scatterings its wave length would be farthest than the initial which is 1216 Å. As we can see in Figure 4.1 the position of the maxima does not change with rotational velocity for the central distribution while for the homogeneous distriution there is a variation in the maxima position X_m for an optical depth $Log_{10}\tau = 5$, this is because at higher rotational velocities photons escape with less scatterings (fig:ref), for $v = 100\,\mathrm{km\ s^{-1}}$the majority of the photons still escape with scatterings (double-peaked line) but for $v = 200\,\mathrm{km\ s^{-1}}$the number of photons that escape with a few or any scatterings is higher (single-peaked line), this is one of the main effects of rotation.

If we now study the effect of the optical depth τ in the maxima position X_m Figure 4.1, we found that as the optical depth increase the maximum position increase and this is a well-known result (include references), we found that this result is not modified by rotation.

Finally when we take into account the viewing angle Fig 2 we found that X_m does not depend on it, but again there is a threshold for the homogeneous distribution in which the double peaked merged into a single peak but this time it is just the angle of viewing effect.

4.2 Full Width at Half Maximum of the Lyman alpha line

The width of the line provide information about the range of the wave lengths of the outgoing photons, in the ideal case in which all the photons escape with the same wave length the outgoing spectrum would be the narrower, therefore as the number of scatterings increase the width increases too (reference).

We use the full width at half maximum (FWHM) in order to study the width of the line for all the models that we propose. We found a dependency of the width with the rotation velocity of the gas cloud, this results are summarize in Figure 4.2. As velocity increase also the equivalent width increase (for both homogeneous and central distribution), it means that some photons escape with fewer scatterings than the static case but at the same time a few photons escape with more scatterings, this can be seen clearly in Figure. (Nscatt)

We also found a dependency with the viewing angles, in particular as the angle increase the width also increase Figure **??**, this was also found in Verhemme et al. 2012 for a rotating disk but the pure effect of rotation can not been study as it is in our case. Following the convention of Verhamme et al 2012 we define $\mu = cos(\theta)$, and we can make

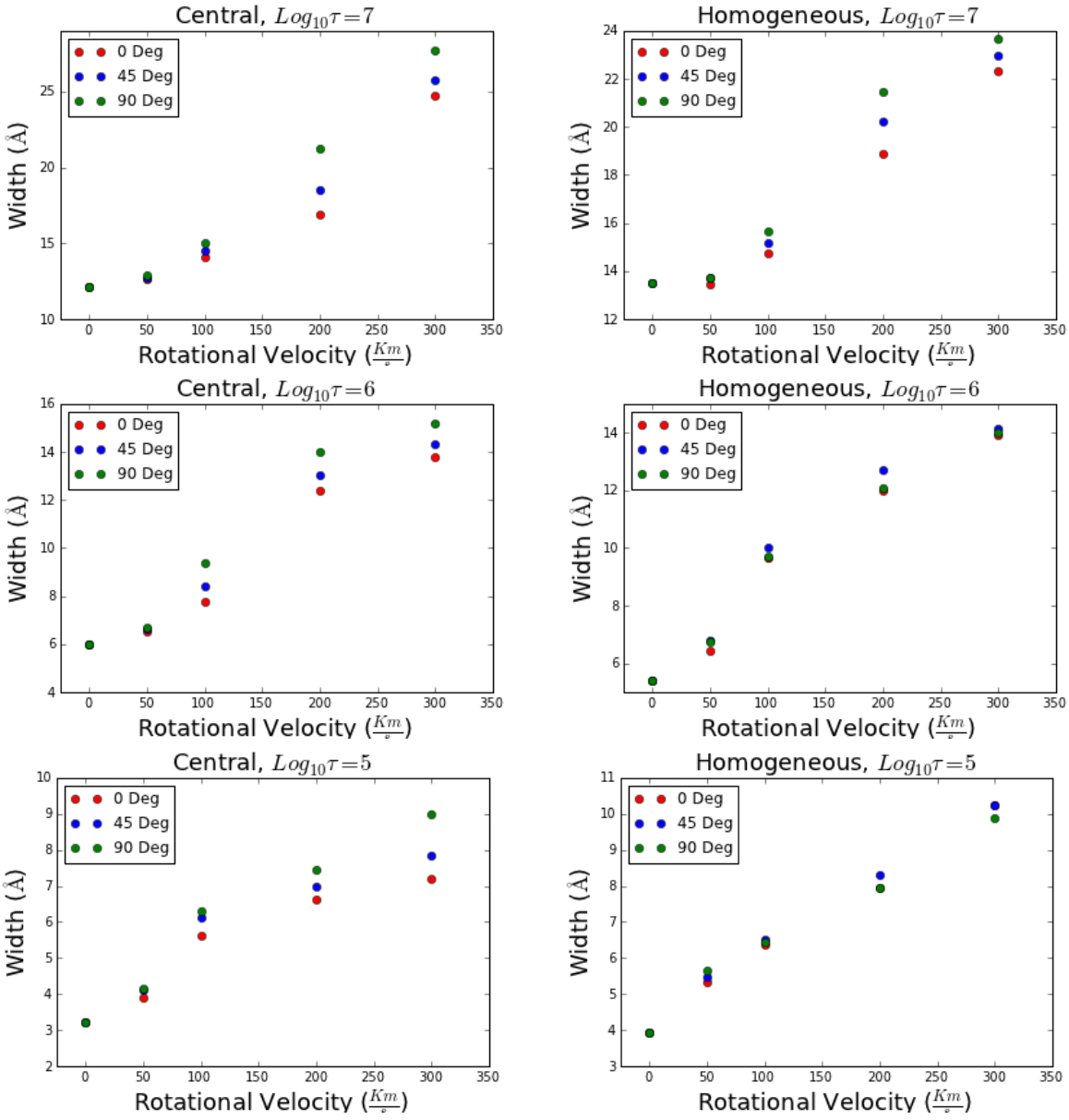

Figure 5. Width of the lyman-alpha line for all the models.

Model	Fit
Central, $\tau = 10^5, V = 200\,\mathrm{km\ s^{-1}}$	$FWHM(\mu) = -149877 + 84509\mu - 17864\mu^2 - 1677\mu^3 - 59\mu^4$
Central, $\tau = 10^6, V = 200\,\mathrm{km\ s^{-1}}$	$FWHM(\mu) = -32264 + 9644\mu - 1080\mu^2 + 53.8\mu^3 - \mu^4$
Central, $\tau = 10^7, V = 200\,\mathrm{km\ s^{-1}}$	$FWHM(\mu) = -1791 + 359\mu - 27\mu^2 + 0.9\mu^3 + 0.011\mu^4$
Hom, $\tau = 10^5, V = 200\,\mathrm{km\ s^{-1}}$	$FWHM(\mu) = -51882.9 + 12932.5\mu - 54.58\mu^2 - 187.22\mu^3 + 11.66\mu^4$
Hom, $\tau = 10^6, V = 200\,\mathrm{km\ s^{-1}}$	$FWHM(\mu) = -7154649 + 2413478\mu - 305268.4\mu^2 + 17158.92\mu^3 - 361.64\mu^4$
Hom, $\tau = 10^7, V = 200\,\mathrm{km\ s^{-1}}$	$FWHM(\mu) = -51074 + 9912\mu - 721\mu^2 + 23.29\mu^3 - 0.28\mu^4$

Table 2. Fits for EW models

a polynomial fit for the $FWHM(\mu)$ for our models, this is resumed in Table 2

4.3 Escape Fraction

The fraction of photons that escape from the cloud of gas and dust is defined as:

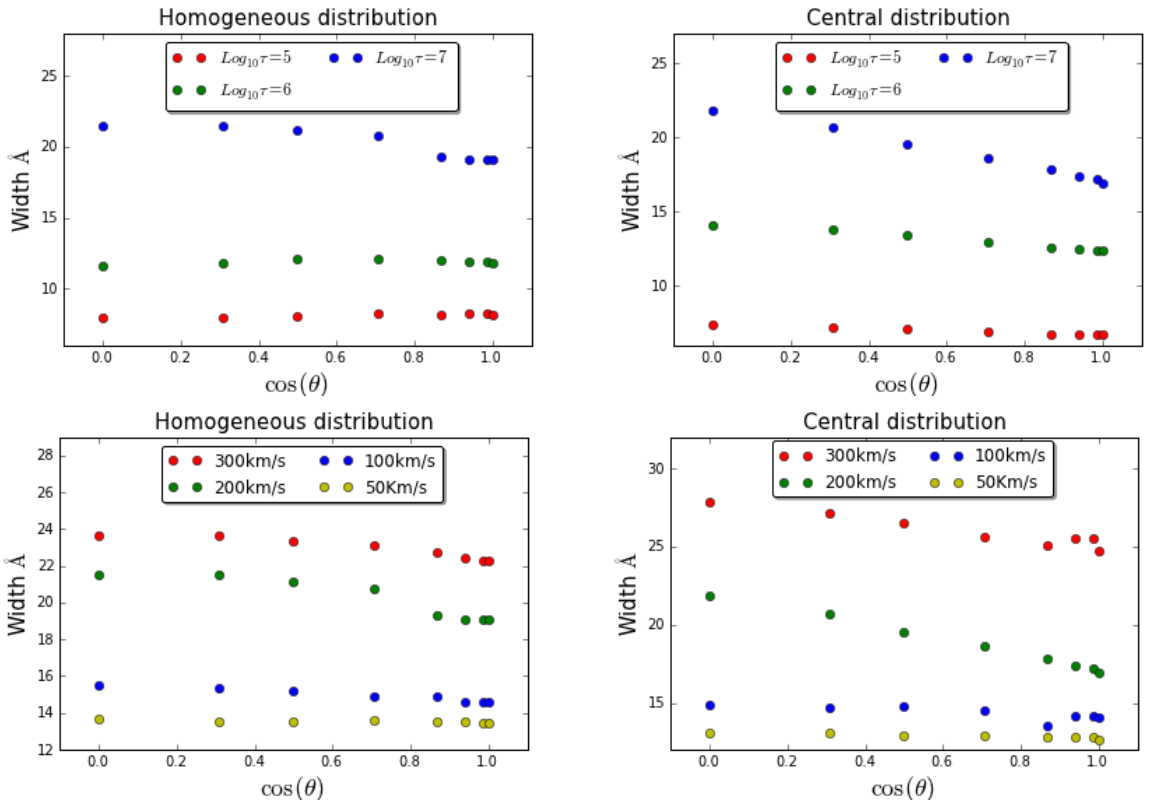

Figure 6. Width of the lyman-alpha line for all the models.

$$F_e = \frac{\Sigma_{NI}\vec{k}\cdot\vec{o}}{\Sigma_{NF}\vec{k}\cdot\vec{o}} \tag{2}$$

Where NI is the initial number of photons and NF is the final, $\vec{k}$ is the rotation axis direction and $\vec{o}$ the observer direction. With this definition we compute the escape fraction for all of our models, the results are shown in Fig 4.3

We found that for the central distribution the escape fraction does not depend in velocity neither in the angle of observation, while it does in the optical depth, this result was already known from previous works (references). On the other hand for the homogeneous distribution we found that for higher velocities photons escape easily. The difference between this two results is due to the fact that in the homogeneous distribution photons are emitted closer to the escape surface and this makes this configuration more sensitive to rotation. This last argument also explain the fact that in the homogeneous distribution the optical depth does not affects the escape fraction .

5 DISCUSSION

6 OBSERVATIONAL IMPLICATIONS

... The results derived in this paper have consequences on the interpreation of galaxy observations in the Lyman alpha line.

Velocity (Km/s)	Maximum 1 position	Maximum 2 position
50	-16.2695	16.23705
100	-15.66496	15.33504
200	-16.93149	14.56851
300	-13.40048	16.09952

Table 3. Optical Depth $\tau = 10^7$, Central Distribution

Velocity (km/s)	Maximum 1 position	Maximum 2 position
50	-7.46286	6.53714
100	-7.53357	6.96643
200	-8.17453	7.32547
300	-6.81487	6.18513

Table 4. Optical Depth $\tau = 10^6$, Central Distribution

7 CONCLUSIONS

ACKNOWLEDGEMENTS

APPENDIX A: TABLES

Line width

Escape fraction

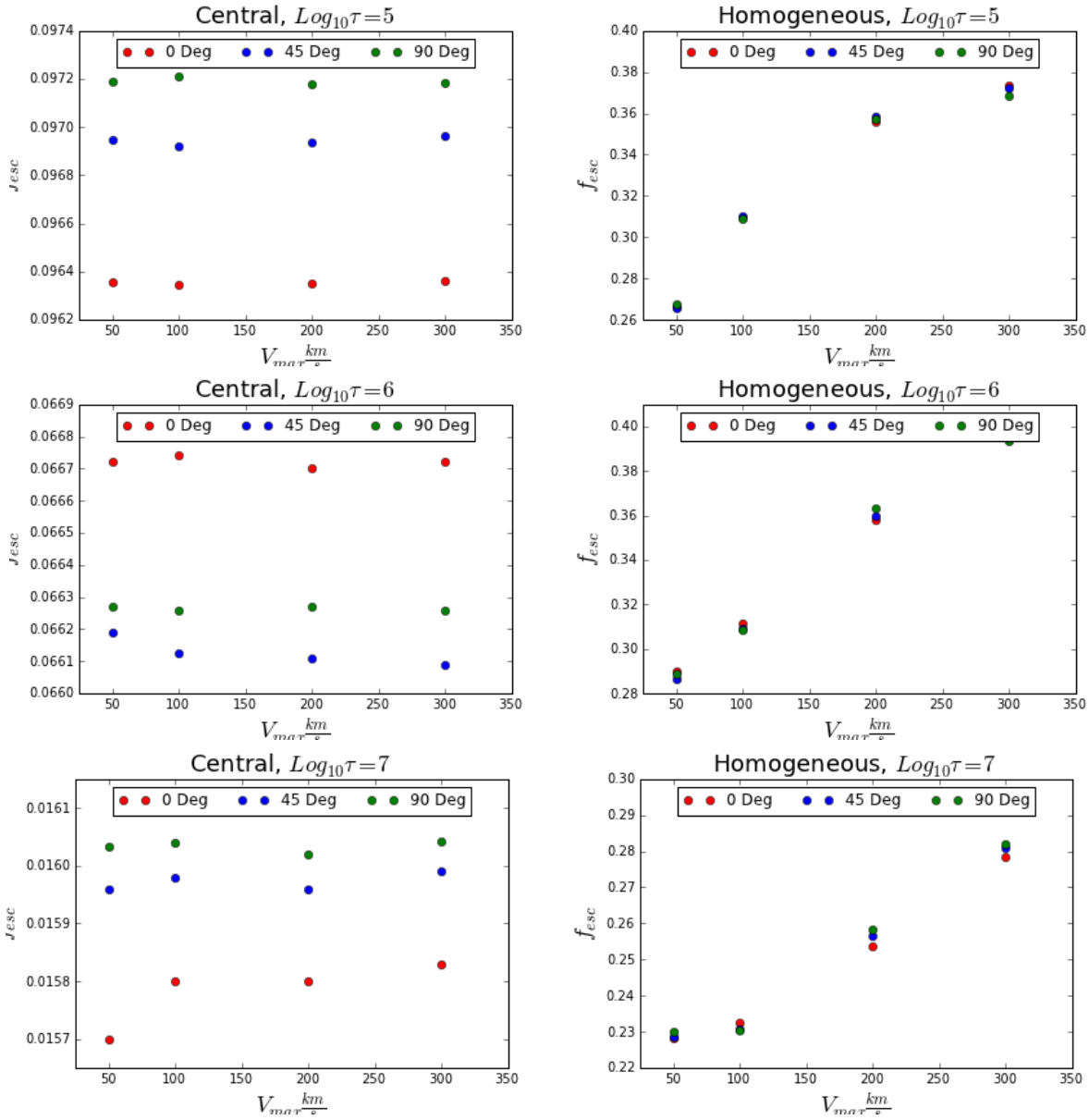

Figure 7. Escape fraction for all the models. Left panels show the central distribution, while right panels show the homogeneous distribution

Velocity(Km/s)	Maximum 1 position	Maximum 2 position
50	-4.33708	3.66292
100	-4.27326	3.72674
200	-3.7737	3.7263
300	-3.84903	4.15097

Table 5. Optical Depth $\tau = 10^5$, Central distribution

Velocity(Km/s)	FWHM	θ
50	12.62	0^o
50	12.72	45^o
50	12.93	90^o
100	14.07	0^o
100	14.48	45^o
100	15.00	90^o
200	16.90	0^o
200	18.51	45^o
200	21.24	90^o
300	24.69*	0^o
300	25.79*	45^o
300	27.73*	90^o

Table 6. Lines Widhts for a Central Distribution and $\tau = 10^7$

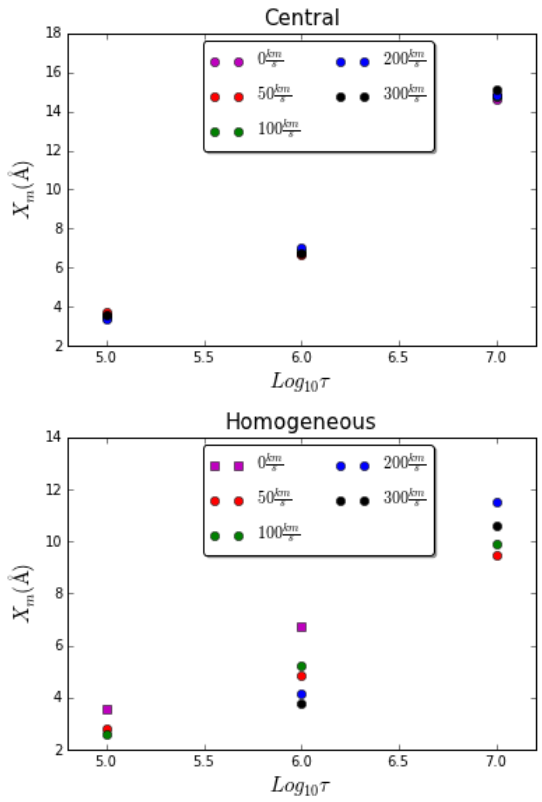

Figure 3. Position of the maxima in the outgoing spectra for differents Optical Depths, (up)Central Distriution, (Down) Homogeneous Distribution.

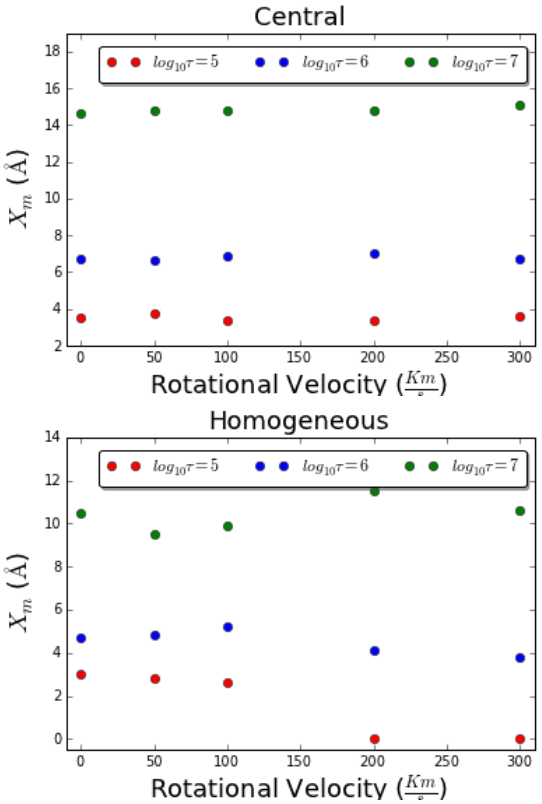

Figure 4. Position of the maxima in the outgoing spectra for differents Rotational velocities, (up)Central Distriution, (Down) Homogeneous Distribution.

[H]

Model	Velocity (km/s)	θ	Dust $\sum(s)$	$\sum(s)$
Homogeneous	50	0^o	13293.06	49939.53
Homogeneous	50	45^o	13291.04	50001.59
Homogeneous	50	90^o	13348.76	49922.73
Homogeneous	100	0^o	15527.69	50114.11
Homogeneous	100	45^o	15511.56	49967.17
Homogeneous	100	90^o	15401.71	49833.65
Homogeneous	200	0^o	17830.85	50078.69
Homogeneous	200	45^o	17932.87	50064.42
Homogeneous	200	90^o	17830.85	49931.748
Homogeneous	300	0^o	18687.33	50048.33
Homogeneous	300	45^o	18572.12	49922.67
Homogeneous	300	90^o	18421.79	49979.37

Table 7. Escape fraction for a Homogeneous Distribution and optical depth 10^5.

Model	Velocity (km/s)	θ	Dust $\sum(s)$	$\sum(s)$
Central	50	0^o	4809.881	49917.069
Central	50	45^o	4829.21	49811.79
Central	50	90^o	4845.108	49853.039
Central	100	0^o	4809.665	49921.30
Central	100	45^o	4828.65	49820.13
Central	100	90^o	4846.45	49854.0
Central	200	0^o	4809.63	49917.64
Central	200	45^o	4829.25	49818.49
Central	200	90^o	4844.89	49856.66
Central	300	0^o	4810.56	49922.98
Central	300	45^o	4831.16	49823.33
Central	300	90^o	4845.33	49858.48

Table 8. Escape fraction for the central Distribution and optical depth 10^5.